RESEARCH ARTICLE OPEN ACCESS

A Portable LIFT Printer to Enable the Fast On-Site Optimization of Inks Toward Special Customer Needs

Stefan Lux[1] | Chaoyu Wu[1] | Christina Salazar[2] | Julian Crespo[3] | Angélica Pérez[2] | Claudio Fernández Acevedo[2] | Dario Mager[1] | Mareen Stahlberger[1] | Daniela Mattes[1] | Laura Weber[1] | Jannik Schlindwein[1] | Clarine Gedigk[1] | Maria B. A. Rosa[4] | Momina Amir[4] | Nadezda Kuznetsova[4] | Michael Kraft[4] | Frank Breitling[1] | Jan G. Korvink[1]

[1]Institute of Microstructure Technology (KIT)—Karlsruhe Institute of Technology, Eggenstein-Leopoldshafen, Germany | [2]Centro Tecnológico Ĺurederra, Los Arcos, Navarra, Spain | [3]Tecnología Navarra de Nanoproductos S.L. (TECNAN), Los Arcos, Navarra, Spain | [4]Department of Electrical Engineering (ESAT), Micro and Nano Systems (MNS), KU Leuven, Leuven, Belgium

Correspondence: Frank Breitling (frank.breitling@kit.edu)

ABSTRACT

Laser-induced forward transfer (LIFT) printing uniquely enables localized deposition of nanoparticle pastes onto target substrates. The extent of its versatility hinges upon the availability of nanoparticle inks that align with the capabilities of the printing device. Given the inherent distinctions among various devices attributed to differences in laser types (continuous-wave or pulsed), laser energy profiles, and adaptable wavelengths, ink formulation and the LIFT printing processes are frequently disjointed, which results in a lengthy optimization cycle. Significantly expedited optimization cycles could be achieved if LIFT performance of an ink could be tested on-site of the ink developer. This localization empowers ink developers to tailor inks precisely to specific usage scenarios by promptly adjusting parameters such as particle size, viscosity, and surface properties. This paper presents a dedicated LIFT device that focuses on fine-tuning ink characteristics and provides insights into the construction to allow other interested researchers to build similar low-cost, user-friendly setups.

1 | Introduction

Laser-induced forward transfer (LIFT) [1] is a versatile printing method, which is well-suited for the deposition of various inks containing nanoparticles. In contrast to other techniques, such as inkjet printing, it presents fewer restrictions regarding the rheological properties of the transferred material. It grants the ability to precisely transfer different formulations, either in close proximity, adjacent to each other, or even in stacked configurations. The fundamental process for transferring liquid or pasty materials via LIFT is illustrated in Figure 1. The potential

applications of LIFT are extensive and have been reported by many different groups, ranging from the creation of functional units [2], over the development of sensors and electrical components, to the synthesis of peptide arrays for disease screening [3, 4] through the targeted combination of diverse materials [5–8]. When a researcher opts to fabricate a sensor using semiconductor nanoparticles such as zinc oxide [9, 10], several challenges must be overcome to obtain optimal printing results. Research groups, thus, typically employ diverse setups [1, 11–13], each optimized or purpose-built for their specific objectives. At least two different transfer mechanisms exist for LIFT printing. One of them

requires an extra laser absorption layer, which is typically made of polyimide to translate the laser pulse into localized heat. Thermal expansion of polyimide then reversibly leads to a "bubble" that touches the underlying acceptor. Simultaneously, the heat melts a few molecular layers at the interface of the to-be-transferred material and the surrounding air that is immediately frozen to the acceptor upon touching it [11]. Therefore, capillary forces and surface tension are active for only a few milliseconds, which, in theory, should increase the chance of printing defect-free and flat nanolayers. The other transfer mechanism works well with nanoparticle pastes and is independent of the laser absorption layer. Laser energy is directly absorbed in the nanoparticle paste, and any liquid component is then evaporated to drive the transfer of nanoparticles to the acceptor [12]. The specific experimental requirements influence the selection of the laser system, with choices ranging from pulsed lasers [14], to continuous-wave diode lasers [11], each offering different energies within the range of 0.05–1.7 J cm^{-2} [12, 15] for pulsed lasers and 0.07–3.6 W (beam diameter of 20–100 μm) [16, 17] for diode lasers. Many different wavelengths have been used for LIFT, varying between 266 and 1064 nm [15, 17]. Just as LIFT setups differ from one another, so do the inks employed in the transfer process. Some groups utilize low-viscosity inks (10–13 mPa s) [18], while others work with high-viscosity pastes (250 Pas) [19]. Dimitrou et al. (2021) already summarized the problem. "Although LIFT has been extensively studied over the past, the same cannot be said for the inks used for LIFT printing. Most researchers employ LIFT with commercially available inks that have not been designed to correspond to the LIFT processing parameter" [20].

To summarize, not every ink is automatically compatible with a particular setup, and the researcher is confronted with a crucial decision—whether to procure a variety of commercially available ink products from established manufacturers (Sigma Aldrich, XTPL, PV Nanocell, etc.) and conduct extensive testing, or embark on the path of developing their own ink. Alternatively, numerical simulations that consider the rheological properties of the ink or high-speed camera analysis of the transfer can aid in the selection or fabrication of inks [21]. However, simulations have difficulties such as complexity, real-world discrepancies, and parameter sensitivity.

To facilitate the approach of ink development, we describe here a simplified version of a portable nano-3D printer to provide researchers with a tool that can be used to evaluate compatibility with the specific setup of tailored ink formulations.

Choosing to formulate the ink in-house provides the flexibility to tailor it precisely for the unique setup and purpose. However, this comes with its own set of challenges, primarily due to the time-consuming nature of the process. Optimization requires a significant investment of time, not only due to the iterative refinement, but also because the ingredients for the ink must either be procured or synthesized. In case of nanoparticle inks, the primary ingredients are nanoparticles, which can undergo various modifications. While fine-tuning an ink by blending pre-existing chemicals poses fewer challenges, the adjustment of nanoparticle formulations is a notably intricate process.

Researchers commonly encounter challenges due to the limited availability of diverse particle sizes or modifications.

Consequently, it becomes imperative for the rapid development of ink to be situated in close proximity to the nanoparticle fabrication facility and its specific know-how. However, not every LIFT laboratory is geographically near such a facility, or equipped with its own nanoparticle production capabilities. This situation results in numerous samples circulating globally and contributes to a slow cycle of ink optimization, in which the development often struggles to keep up with evolving demands.

To address this challenge, the development of a convenient screening device for ink optimization is essential. This device should be straightforward to build as a user-friendly machine, focusing on its primary function of facilitating LIFT ink optimization. The present paper aims to demonstrate the construction and adaptation of such a device to meet the specific requirements of a customer's LIFT system. The device is designed to be compact and mobile with a cost approximately equivalent to that of a single ink purchase in the market (currently approximately 500€). The paper will showcase how this simplified device can be effectively used for in-house optimization of nanoparticle inks. The uncomplicated nature of the device allows for multiple cycles of adaptation for key ink properties within a few weeks. The final optimized product is then tested in the main LIFT setup to demonstrate its usability. For the characterization of electrical properties, a small structure is printed, providing valuable insights into the performance of the developed ink.

2 | Results and Discussion

2.1 | Portable LIFT Setup

The portable LIFT setup was devised to facilitate ink optimization at remote locations, mainly on-site or near nanoparticle fabrication facilities. Consequently, it was designed to be compact, lightweight, and easily transportable. This objective was attained by streamlining the device to its essential components. Although cost reduction was not the primary focus, achieving this goal offered the added benefit of being an economical solution. At the time of writing, all components could be procured off-the-shelf for less than 500€. Figure 2a illustrates the fully functional device, which occupies only half a desk space. The setup is based on a commercially available and low cost CNC machine with its milling head replaced by a laser source. This provides an x–y-platform with which to move a laser beam over desired locations. As depicted in Figure 2b, the optical pathway remains straightforward, with the laser beam being directed through a collimator lens onto the substrate. While this simplicity imposes limitations, such as the minimum laser spot diameter and its energy distribution, it does not compromise the device's efficacy as a tool for characterizing inks. The transfer process is driven by a locally heated polyimide foil, expanding in the z-direction towards the receiving substrate. For safety purposes, a laser-tight cover box was installed which could be opened between transfer cycles. This box shielded the operator from harmful laser radiation and enabled safe operation in conjunction with an interlock system. The controller electronics was housed within a protective enclosure that only required opening for reprogramming, a step typically unnecessary, as depicted in Figure 2c,d. The transfer protocol was pre-programmed and could
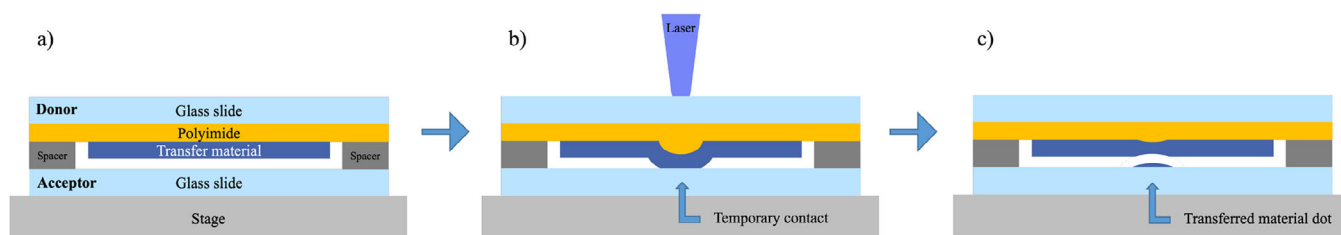
FIGURE 1 | (a) A laser-transparent glass slide is covered with adhesive polyimide tape and a thin layer of transfer material, positioned above a second slide. The receiving substrate is in close proximity, separated by a spacer. (b) The laser beam is directed onto the donor substrate, and its energy is absorbed by the polyimide, causing it to expand towards the receiving substrate until in contact. (c) Subsequently, the polyimide retracts, leaving behind a small amount of transfer material on the receiver.
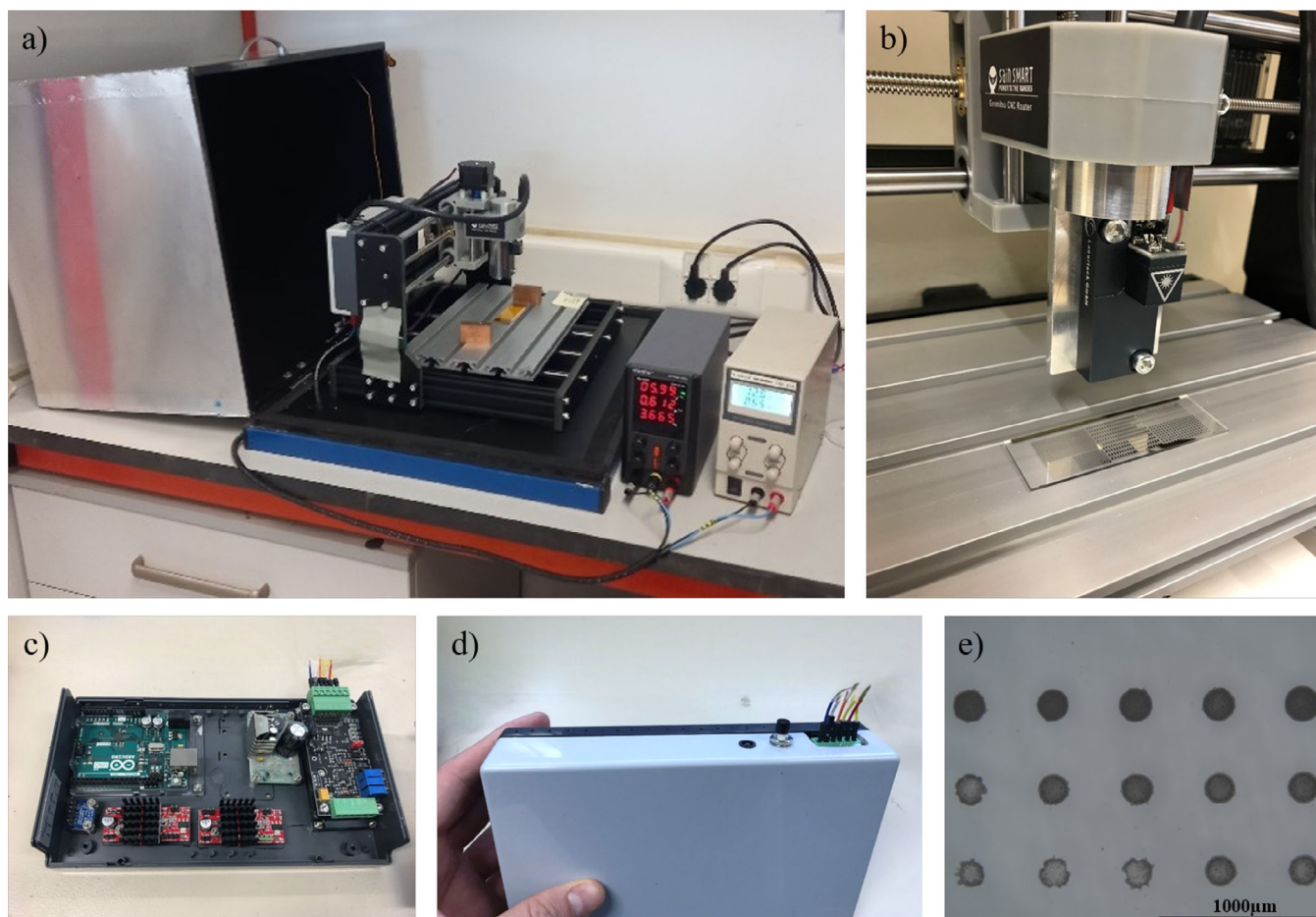

FIGURE 2 | (a) The mobile LIFT printer used rapid on-site evaluation of ink candidates and applied in an ink development processes. (b) Exchangeable laser module of a 405-nm diode laser and paired acceptor slide. (c) The electronic components of the mobile LIFT setup include an Arduino Uno, a voltage converter, a laser driver unit, X- and Y-axis stepper drivers, and a moderately fast digital-to-analog converter. Reprogramming exclusively necessitates access to its enclosure box. (d) Streamlined controls facilitate effortless operation of the device, with a single button initiating the LIFT transfer process, following a predefined protocol. (e) The successful LIFT printing of an ink candidate, developed with the assistance of the mobile LIFT setup, is here demonstrated.

be initiated with the simple push of a button. After a countdown, the machine started the transfer when the cover was closed. This user-friendly design facilitated operation for individuals without expertise in machine coding or electronics. Figure 2e illustrates the successful transfer of an ink candidate optimized with the portable LIFT setup. A more detailed description and circuit diagram of the device can be found in the supplementary section.

2.2 | Modification of Viscosity

To demonstrate how the implementation of our LIFT device could help streamline the optimization of a nanoparticle ink, we employed the device to find an optimal formulation of a ZnO nanoparticle paste in order to develop a method for all-inorganic printed sensors. Our team consisted of three groups, one that focused on the technology and application side, and
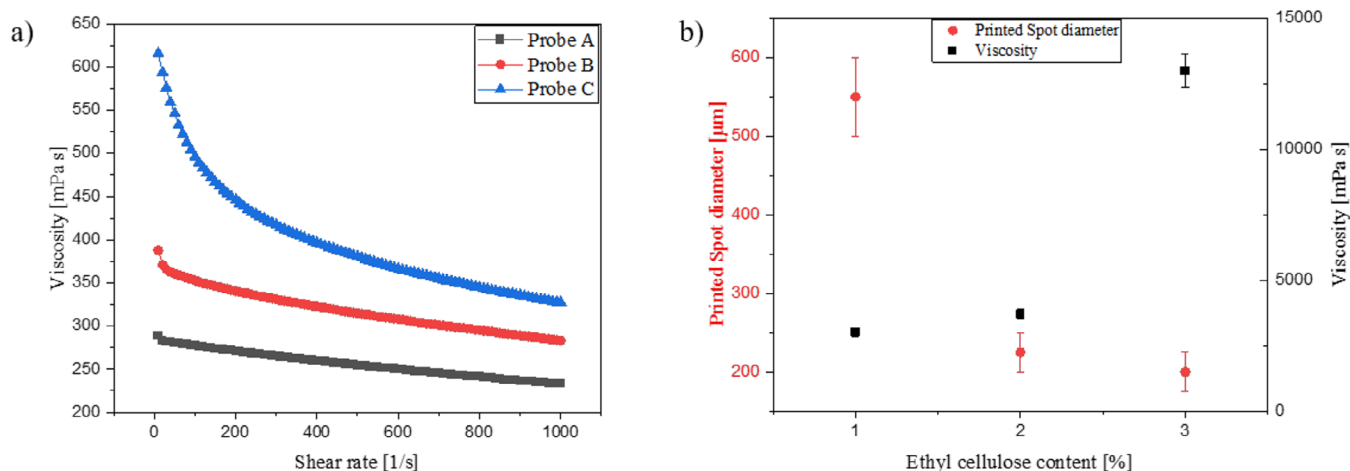
FIGURE 3 | (a) Viscosity measurements were conducted on three zinc oxide (ZnO) pastes containing different concentrations of ethyl cellulose across a range of shear of 0–1000 L s^{-1} using a parallel plate geometry. Each paste exhibited varying degrees of shear thinning behavior, with Sample C demonstrating the most pronounced effect, and Sample A the least. This phenomenon is linked to the lower presence of ethyl cellulose polymer chains in Sample A, resulting in reduced resistance to flow under shear stress, and less pronounced shear thinning behavior. (b) Elevating the ethyl cellulose content lead to an increase in viscosity. Simultaneously, the reduction in the printed spot diameter occurred due to enhanced structural recovery.

situated in Germany, and two teams of ink-developing experts in Spain working closely together. To identify the ideal paste parameters, the device developed in Germany was provided to the cooperation partners in Spain to enable on-site optimization, with a short duration of each iteration. The final ink was then shipped to Germany and tested on a larger setup for its applicability to print small dots.

The ZnO paste was prepared by dispersing ZnO nanoparticles in a solution containing polyvinyl pyrrolidone (PVP) and 2-butoxyethanol, followed by the addition of ethyl cellulose. Both PVP and ethyl cellulose acted as dispersing agents and binders. The viscosity of the paste was primarily influenced by the concentration of particles and binders, whereby higher concentrations led to increased viscosity and vice versa. The interplay among these components significantly affected the flow characteristics, ultimately influencing the printed structure.

To modify the viscosity, the content of ethyl cellulose in the ink was adjusted from 1 % to 3 %. The ink with modified viscosity was then evaluated for its printing properties, revealing a correlation between viscosity and spot diameter, as illustrated in Figure 3b. This study additionally identified a lower viscosity limit at 100 cPs = 100 mPas below which no transfer with our device was feasible. Within the range of 100–3000 cPs, or 100–3000 mPa s transfer was possible, but spot divergence became pronounced. Above 3000 cPs = 3000 mPas, numerous suitable ink candidates could be identified.

2.3 | Modification of Nanoparticle Concentration

Adjusting the nanoparticle concentration serves as another means to fine-tune the rheological printing parameters of the ink. By manipulating the weight percent of nanoparticles, one can effectively alter the ratio of organic solvent to solid components. Consequently, a higher solid content induces an increase in

viscosity, and thereby can influence the size of the printed spots. Tailoring the particle content is crucial, aligning with the unique requirements of users. In specific cases, opting for a lower particle content becomes preferable, especially when aiming to achieve a more porous structure post-sintering. This is particularly relevant for applications such as printing of gas sensors, where enhanced porosity plays a pivotal role in optimizing performance [22]. Then again, in other scenarios, a more bulky structure is essential, such as when aiming to maximize conductivity [20].

2.4 | Further Optimization Perspectives

This study primarily focused on investigating the particle concentration and viscosity of the ink candidates to demonstrate the usefulness of the device. However, additional parameters were also examined, including variations in organic solvents and particle size. Inks containing progressively smaller particles (<77 nm) were excluded during optimization due to unsuccessful transfers. Conversely, inks formulated with larger particles (>191 nm) demonstrated improved transfer conditions. Regarding solvent variation, inks using 2-butoxyethanol and diethylene glycol monoethyl ether (DEGMME) were investigated. While samples with 2-butoxyethanol could be transferred without visible agglomerations (see Figure 4), those formulated with DEGMME exhibited transferable structures, albeit with visible agglomerations (see Supplementary Information). Further exploration could involve experimenting with different elemental combinations of nanoparticles, incorporating shell structures, or utilizing nonspherical particles. In addition to the optimization of recipes for the production of pastes, further adjustments could also be made to improve the LIFT process. For example, better control of the transfer temperature in coordination with the inks could lead to improved drying behavior. A small extension of the LIFT setup for temperature control could be integrated into the table for this purpose. These avenues hold promise for future studies and warrant further investigation.
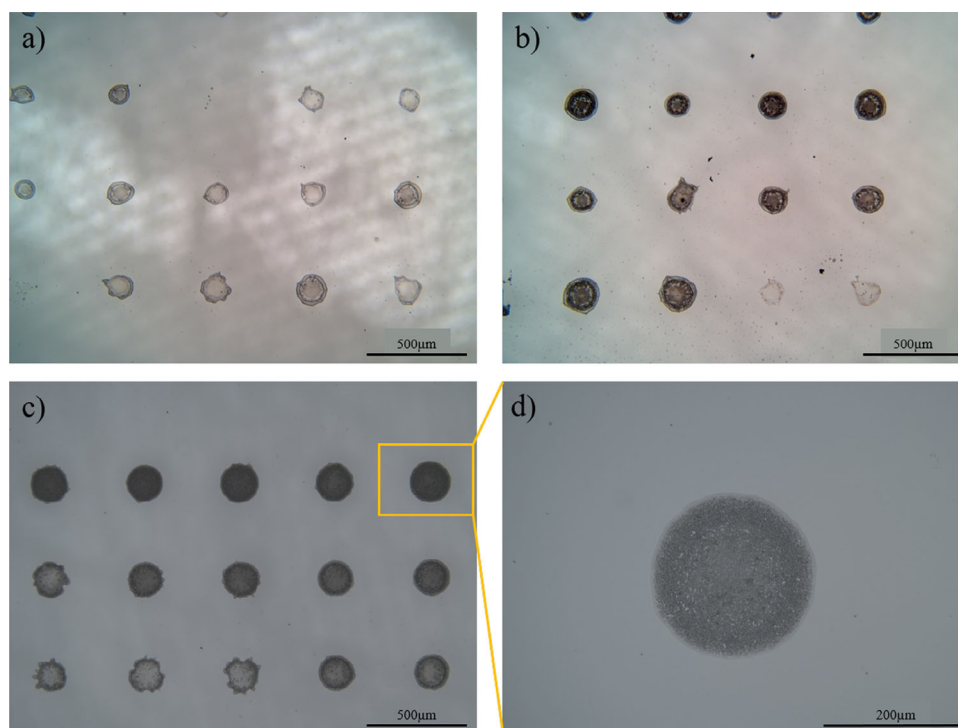
FIGURE 4 | A small screening of optimum laser parameters was done for paste candidates A, B, and C at the customer's laboratories. A horizontal row of five spots increases the laser power in 20 mW steps from 220 to 300 mW. The vertically spaced rows vary the laser duration in 2-ms steps from 6 to 10 ms. (a) LIFT printing of paste candidate A with the lowest viscosity 2900 mPa s. (b) LIFT printing of paste candidate B with medium viscosity 3800 mPa s. (c) LIFT printing of paste candidate C with the highest viscosity 6100 mPa s. (d) Detailed view of a single fairly uniform spot of paste candidate C shows the distribution of material within the spot.

3 | Test of Paste Candidates

Various paste candidates were manufactured and optimized with the portable test device on-site at the project partner's location in Spain. The final inks were then used with the LIFT production printer by the group in Germany. The paste candidates were optimized with respect to particle size, particle concentration, and viscosity. Three promising candidates were subsequently selected based on the on-site test results obtained using the portable LIFT device. The criteria for selection included general printability, transfer quality concerning nanoparticle distribution, dot roundness, and consideration of spatter and spillage possibilities. The three candidates are indicated as A, B, and C, where A was the ink with the lowest particle content of 1–10 mg mL^{-1}, B with 25–50 mg mL^{-1}, and C with 150–200 mg mL^{-1}. In addition, the viscosity of paste candidates was measured and is shown in Figure 3a. The figure illustrates the viscosity as a function of the shear rate. Sample C showed the highest viscosity, which was taken into account for the selection of the best paste. At the Karlsruhe Institute of Technology (KIT), home to the production LIFT printer for which ink optimization was conducted, the preparations for the transfer process were carried out. Through experimental analysis, we determined that doctor blading with a blade height of 40 μm ensured a successful transfer. From empirical data, we determined that a spacer of 90 μm between the donor and acceptor was an optimal choice to prevent undesired transfer or sticking between the donor and acceptor, ensuring the desired transfer at locations heated by the laser. A screening for the optimum laser parameters was conducted, varying both the laser exposure and laser power to identify the optimal combination. The criteria for selection included achieving reliable spot transfer with round spots, a uniform distribution of ink, and no spattering. Roundness was evaluated by comparing the spot diameters in the *x*- and *y*-directions. The transparency of the spot was a good indicator of the uniformity of the ink distribution; however, the assumptions were additionally supported by vertical scanning interferometer (VSI) measurements (see Figure 5 and Supporting information).

Figure 4a,c illustrates the screening for the best laser parameters. A favorable set of parameters was identified in the top right corner, featuring high laser energy (300 mW), and a short laser duration (6 ms). Figure 4d provides a more detailed view of the selected parameters.

The topographic data of the VSI (see Figure 5) show an ink distribution that is typical for the drying of printed materials, owing to the coffee staining phenomenon [23]. The fluctuation in the graph is likely due to the reflective properties of the material. Existing strategies can be used to reduce the coffee ring effect and improve the homogeneous distribution of nanoparticles, such as increasing the viscosity to suppress flow, adding surfactants or using a mixture of high and low boiling point solvents for ink fabrication [24–26]. These measurements demonstrate that the device has great potential for making ink development for nanoscale printing more effective by shortening the optimization cycles. Even though the dried material dot measured an average height of 260 nm, this was reduced to 70 nm by sintering, and thus truly matched the nanoscale. In the future, these inks could be used in printed electronics in the form of insulators,
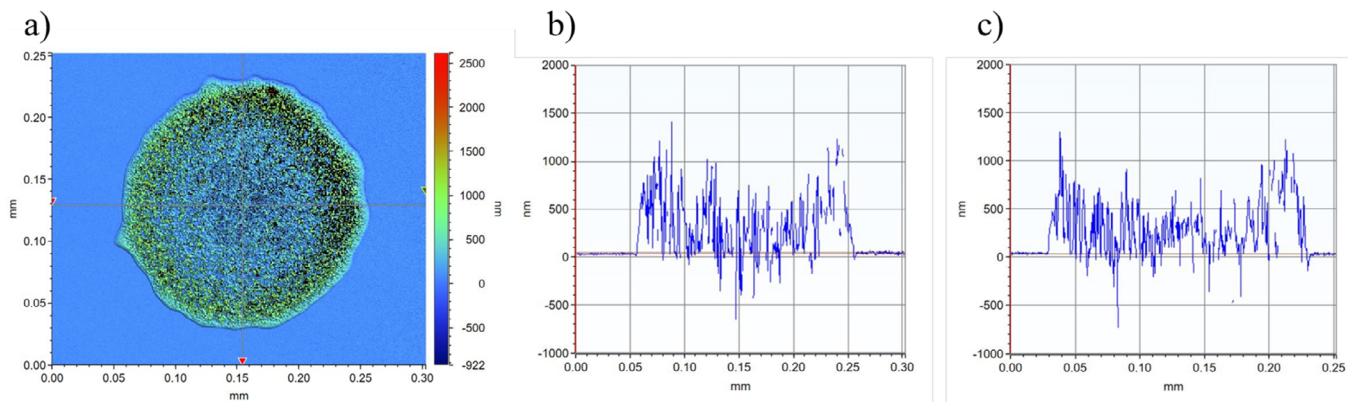
FIGURE 5 | Analysis by vertical scanning interferometry for the printed material spot of paste C with the transfer parameter 280 mW and 6 ms. (a) Indication of topographic height distribution by color scheme. (b) X profile at the center of the spot. (c) Y profile at the center of the spot.

as gas sensors or as thin dielectrics for capacitors. The ability to print, combine, and stack various materials in nanometric layers opens many possible applications. With programming knowledge, the test device could also be used as a fabrication device with compromise regarding precision and printing speed in comparison to a fabrication device.

4 | Conclusion

The mobile adjustable LIFT setup facilitated the efficient and cost effective optimization of customized inks at the ink development site, without necessitating extensive iterations and testing by the end-user. This on-site ink optimization process offered immediate feedback on whether a particular product aligned with the specified conditions or should be rejected. The optimization and fabrication cycle could be significantly reduced from months or years to a matter of weeks.

In the conclusive test conducted at the Karlsruhe Institute of Technology (KIT), the "customer" demonstrated the successful selection of inks by TECNAN as the "manufacturer." The manufacturer's investment requirement was limited to adapting the mobile LIFT setup in accordance with the customer's specific needs.

At both setups, similar results were observed regarding the selection of printable ink candidates. While all inks showed drying effects, especially for low viscosity inks, ink candidate C revealed the most homogeneous spots in terms of roundness and particle distribution.

For paste production, an effective combination of key ingredients was identified. Viscosity adjustment was achieved by precisely controlling the amount of ethylcellulose. Our measurements revealed that viscosity plays a pivotal role in achieving smaller spot sizes, denoted as lateral size. The concentration of nanoparticles also significantly influenced ink optimization, with the goal varying depending on the intended application—aiming for either higher or lower concentrations in the final product.

It is essential to note that the modification of nanoparticle concentration had a consequential impact on viscosity. Therefore,

an optimum concentration must be chosen based on the specific application. Due to the easy fabrication and low cost of the LIFT-setup, this device can be implemented by other manufacturers in the future to effectively streamline the selection process of NP-formulations for LIFT printing in order to reach the goal of LIFT-printed flat all inorganic nanolayers.

5 | Materials and Methods

5.1 | Laser-Induced Forward Transfer

The application of LIFT allows for the localized transfer of diverse materials. In our study, the LIFT system was employed specifically for the transfer of pasty materials using a diode laser. This process involved directing the laser beam through the relative movement of the laser diode and the substrate table, focusing it onto a donor substrate using an integrated collimator lens. The donor and acceptor slides were vertically stacked in close proximity but were separated by a precisely defined spacer, as illustrated in Figure 1. Typically, rolled steel with a thickness ranging from 70 to 90 μm was used, although the actual thickness could vary depending on the layer thickness of the transfer material. The donor slide was composed of laser-transparent microscope glass, coated with the material intended for transfer using a doctor-blading technique. The laser induced localized heating in the donor material, resulting in the transfer of material spots onto the acceptor substrate. The acceptor, typically another microscope glass, could alternatively be replaced with substrates such as silicon or flexible polyimide film. In cases where polyimide was used as the actuating material, the laser's heat was absorbed by the polyimide film, causing a short expansion in the z-direction, and thus forming material contact between the donor and acceptor slides. This rapid process left behind a material dot on the acceptor. The size of the transferred material dots was controlled by adjusting the laser power and exposure time, which acted as the driving force behind the expansion in the z-direction.

5.2 | Donor Preparation

The preparation of donors involves the creation of a thin and uniform layer of transfer material on a carrier substrate with

a typical thickness ranging from 20 to 50 μm. The donor was considered uniform when it appeared consistent in composition, and exhibited the same thickness throughout. In this study, doctor blading was used for the fabrication of layers.

The donor preparation process started with cleaning microscope glass slides sequentially in an ultrasonic bath containing soap water, deionized water, isopropanol, and finally acetone. The slides were made of soda lime glass, which is transparent to visible light, including the laser irradiation of 405 nm used in the subsequent steps. The glass slides were cleaned to remove any dust or residuals from the manufacturing process. After cleaning, adhesive polyimide tape was applied to the glass slides. The polyimide tape consisted of a thin polyimide layer with an additional layer of polysiloxane glue. It served as an absorbing layer for the laser pulse and was necessary when working with nonabsorbing transfer materials.

Next, a film applicator was used for the donor preparation. The sled or blade of the applicator was adjusted to a precise height above the substrate, and the transfer material was distributed onto one side of the glass-polyimide stack. The film applicator moved the sled along the length of the glass slide at a constant speed, resulting in a donor with a defined thickness that was uniformly covered with the transfer material. The quality of the donor preparation was assessed visually through transparency and surface roughness. All donors were prepared with a theoretical layer thickness of 40–50 μm defined by the gap between substrate and blade. However, the actual thickness of the coating could vary due to process limitations.

5.3 | Portable LIFT Setup

The portable LIFT printer was designed as a simplified setup that was reduced to its basic functions, such as having a controlled laser and an x-y-positioning capability w.r.t. the receiving substrate. Reduced to its basic functions, it could be used as a tool for optimizing the ink fabrication. Important aspects were its relatively small size, high mobility, and affordable price. The individual components were easily accessible and could be replaced or adjusted to meet the specific requirements of each ink user.

The LIFT ink printer was constructed out of three main units, which worked together as a functional LIFT system. The electronic circuit diagram and Arduino code can be found in the supporting information.

The first unit was the mechanical stage, based on a CNC milling machine by SainSmart [27]. The model Genmitsu 3018 Pro [28] offers a mechanical platform that was originally designed to control a milling head within a 300 mm × 180 mm area. Its motor was replaced by a small diode laser, forming the functional unit of the LIFT printer.

Other mechanical platforms, such as FDM-3D-printers, or engravers, would also have been suitable for this purpose and had already been demonstrated [16]. The main reason for choosing the CNC machine was to ensure maximum flexibility and accessibility of the components. Popular 3D filament printer platforms would be conceivable extensions when targeting high, nonflat substrates.

The relative movement of the laser above the sample was controlled by stepper motors, one for the movement of the platform in x-direction and one for the movement of the laser in y-direction. The stepper motors offered 0.25 nm of torque which is enough for mechanical milling and proved ample for the planar positioning of the laser. As a testing device for LIFT materials, precision in the x–y-plane of approximately 10 μm was necessary, given that the expected spot diameter ranged from approximately 100 to 200 μm, with a pitch of around 300–500 μm. The stepper motors could be operated in a microstep mode, which was translated via a threaded rod to achieve a theoretical step size of 2.5 μm, without accounting for the inevitable mechanical tolerances.

A third stepper motor controlled the z-position of the laser and was used to adjust the focal plane of the laser onto the transfer substrate. Typically, this adjustment was performed just once during the assembly and testing of the LIFT device and did not require regular alterations. For the sake of simplicity, the motor controls were not integrated into the self-built control unit, despite their feasibility. Instead, the available original CNC control electronics were utilized, providing a user-friendly interface for adjustment of the laser height. This approach proved to be the simplest, given that the device's primary objective was transferring onto microscope glass substrates. For increased flexibility in substrate selection, integrating z-control for rapid adaptation would be advisable.

The second main component in our setup was the laser source, specifically a diode laser from Lasertack GmbH, 34277 Fuldabrueck, Germany. The laser was selected for its compact size and precise emission control. Choosing this supplier provided versatility in both wavelength and power output. Users could select from 12 emission wavelengths ranging from 405 to 830 nm, with power outputs varying from 0.03 to 6w. In our setup, we utilized a 405 nm and multimode 500 mW diode laser to closely match the wavelength and power specifications of the production printer. The manufacturer specified a wavelength range of 398–410 nm; however, we assumed that for localized heating, minor wavelength deviations are not relevant and the laser energy is still absorbed by the polyimide layer. While other suppliers may offer an even wider ranges of wavelengths and power options, Lasertack lasers were distinguished by their compact design and uniform base platform. This standardization facilitated easy interchangeability of lasers within our experimental setup.

Exploration of alternative laser types and configurations is viable with modifications to the experimental setup. For larger laser assemblies, structural reinforcement of the framework may be imperative. Moreover, for motorization, it would be advantageous to stabilize the laser and exclusively manipulate the sample along the x–y-axis, but such CNC machines or 3D printers are uncommon. An alternative design concept, often used in IR-laser cutter plotters, involves the manipulation or translation of a set of mirrors to redirect the laser beam, eliminating the need for direct movement of the laser source.

To initially adjust the laser focus, the collimator lens integrated into the laser diode module was positioned. The optical focal

length is 81 mm. The objective was to achieve a laser focus that closely resembled that of the primary LIFT system, which utilizes an f-theta lens to focus the laser beam onto the substrate, resulting in a laser spot diameter of approximately 40 μm. However, it should be noted that the simplified LIFT setup may not attain a laser spot size as small, but rather approximately 80 μm. The spot diameter was determined by measuring the burn marks on the polyimide films. Nevertheless, the printing results were considered sufficiently applicable for our purposes. If we consider the LIFT process as a rapid, spot-localized heating and expansion of polyimide, the deposited energy integrated over time per area becomes an important factor. Differences in energy density can be adjusted by varying the laser pulse exposure or laser power at the primary system, if necessary. Due to the larger laser spot size, a larger material spot is then expected. For focus adjustment, this involves striving to achieve the smallest possible spot size within the polyimide layer of the donor slide. Following a coarse adjustment of the lens to focus on the donor layer, fine-tuning was performed by incrementally adjusting the height of the laser module using the z-motor. This minimum size could be determined either by utilizing an image sensor or by simply examining the burn marks on the polyimide after testing. The laser diode was controlled with a laser driver module provided by Lasertack. The laser driver controlled the emission of the laser by applying voltage and current to the diode according to a modulating voltage received by the LIFT control unit. Although the laser diode was calibrated by the manufacturer, a calibration check was performed. Thorlabs Thermal Power Sensor Head Model S401C was used to verify that the laser source could be adjusted precisely within the range of 0–500 mW.

The third unit was the LIFT control unit, which contained all electronics housed together in a compact box. Not only the laser driver, but also the x–y-motor drivers were closely packed together, reducing any wiring and sources of disruption outside of the box. To manage the many different voltage requirements, including 12 V for the laser driver, 5 V for the microcontroller and the DAC, and 6–9 V for the stepper drivers, an additional voltage converter type H-tronic 115967 was integrated. A programmed Arduino Uno micro controller formed the heart of the machine and controlled all separate units. The goal was to simplify the design of the machine by keeping in mind that the operator was unlikely to be a machine programming expert. A simple button to start the machine, placed on the outside of the box, and an indicator LED, formed all the controls that were necessary for testing pastes with the machine. The Arduino Uno was preprogrammed, and ran its code after the start signal was given by pressing a button. The open source code and the circuit diagram are found in the supplementary section. The code communicated with the drivers and moved them to predefined positions before turning the laser on and off for a short pulse. While the motor drivers were connected directly to the Arduino, the laser driver would read an analog voltage signal. Because the Arduino Uno is not capable of generating such a signal, an additional digital-to-analog-converter (DAC) type MCP4725 was connected to the SDA-SCL port. For future designs, the use of a microcontroller with a true analog output, such as the Arduino Uno R4, is recommended and would make the DAC obsolete.

The printing pattern, position, laser power, and duration were adjusted to match the primary LIFT printer, which in this case was a 300-mW diode laser. With the intention to achieve comparable results, the mobile LIFT printer should operate in the same energy region. An exact value for the transfer could not be determined and depended on the paste candidates, therefore, an energy range was tested from 160 to 280 mW, with a laser pulse duration of 10 ms. Because the transfer of a single material dot was not very significant, a pattern of 16 identical dots was transferred for each energy parameter, in steps of 20 mW, transferring a pattern of 96 dots. (The 260-mW parameter was skipped because of limited space on the acceptor slide.) This dot pattern could be analyzed for each paste candidate to determine if a material can be transferred, its lower energy limit, as well as its reliability. This screening method for suitable printing parameters enabled efficient and fast testing of ink candidates. One test cycle took about 3 min, so approx 2 s per dot. The printing quality could be evaluated by examining the spot morphology with a light microscope. To determine the height or other material properties, further methods, such as VSI and other, could be applied.

As shown in Figure 2, the device was covered in a laser-tight enclosure to avoid the risk of potential eye damage. The laser cover was connected to an interlock system, avoiding any unwanted laser emission, making the printer safe to be used even by untrained personnel.

Conflicts of Interest

Prof. Dr. Frank Breitling is a shareholder of PEPperPRINT GmbH, Heidelberg, a company that uses the LIFT system for peptide array production. The other authors declare no conflicts of interest.

Data Availability Statement

The data that support the findings of this study are openly available in KITopen at https://10.35097/NCRGATMjRaFoCzBA , reference number 1000172564.

References

1. P. Serra and A. Piqué, "Laser-Induced Forward Transfer: Fundamentals and Applications," *Advanced Materials Technologies* 4, no. 1 (2018): 1800099, https://doi.org/10.1002/admt.201800099.

2. J. S. Stewart, T. Lippert, M. Nagel, F. Nüesch, and A. Wokaun, "Red-Green-Blue Polymer Light-Emitting Diode Pixels Printed by Optimized

Laser-Induced Forward Transfer," *Applied Physics Letters* 100, no. 20 (2012): 203303, https://doi.org/10.1063/1.4717463.

3. A. Piqué, R. Auyeung, J. Stepnowski, et al., "Laser Processing of Polymer Thin Films for Chemical Sensor Applications," *Surface and Coatings Technology* 163–164, (2003): 293–299, https://doi.org/10.1016/s0257-8972(02)00606-0.

4. L. Rapp, C. Constantinescu, Y. Larmande, et al., "Functional Multi-layered Capacitor Pixels Printed by Picosecond Laser-Induced Forward Transfer Using a Smart Beam Shaping Technique," *Sensors and Actuators A: Physical* 224 (2015): 111–118, https://doi.org/10.1016/j.sna.2015.01.020.

5. F. Di Pietrantonio, M. Benetti, D. Cannatá, et al., "Volatile Toxic Compound Detection by Surface Acoustic Wave Sensor Array Coated With Chemoselective Polymers Deposited by Laser Induced Forward Transfer: Application to Sarin," *Sensors and Actuators B: Chemical* 174 (2012): 158–167, https://doi.org/10.1016/j.snb.2012.07.106.

6. C. Boutopoulos, C. Pandis, K. Giannakopoulos, P. Pissis, and I. Zergioti, "Polymer/Carbon Nanotube Composite Patterns Via Laser Induced Forward Transfer," *Applied Physics Letters* 96, no. 4 (2010), https://doi.org/10.1063/1.3299004.

7. F. F. Loeffler, T. C. Foertsch, R. Popov, et al., "High-Flexibility Combinatorial Peptide Synthesis With Laser-Based Transfer of Monomers in Solid Matrix Material," *Nature Communications* 7 (2016), 11844, https://doi.org/10.1038/ncomms11844.

8. G. Paris, D. Bierbaum, M. Paris, D. Mager, and F. F. Loeffler, "Development and Experimental Assessment of a Model for the Material Deposition by Laser-Induced Forward Transfer," *Applied Sciences* 12, no. 3 (2022): 1361, https://doi.org/10.3390/app12031361.

9. A. Sarkar, S. Maity, P. Chakraborty, and S. K. Chakraborty, "Synthesize of ZnO Nano Structure for Toxic Gas Sensing Application," *Procedia Computer Science* 92 (2016): 199–206, https://doi.org/10.1016/j.procs.2016.07.346.

10. D. Yang, A. G. Ramu, Y. Lee, et al., "Fabrication of ZnO Nanorods Based Gas Sensor Pattern by Photolithography and Lift Off Techniques," *Journal of King Saud University —Science* 33, no. 3 (2021): 101397, https://doi.org/10.1016/j.jksus.2021.101397.

11. G. Paris, A. Klinkusch, J. Heidepriem, et al., "Laser-Induced Forward Transfer of Soft Material Nanolayers With Millisecond Pulses Shows Contact-Based Material Deposition," *Applied Surface Science* 508 (2020): 144973, https://doi.org/10.1016/j.apsusc.2019.144973.

12. P. Serra, M. Duocastella, J. Fernández-Pradas, and J. Morenza, "Liquids Microprinting Through Laser-Induced Forward Transfer," *Applied Surface Science* 255, no. 10 (2009): 5342–5345, https://doi.org/10.1016/j.apsusc.2008.07.200.

13. S. Eickelmann, S. Moon, Y. Liu, et al., "Assessing Polymer-Surface Adhesion With a Polymer Collection," *Langmuir* 38, no. 7 (2022): 2220–2226, https://doi.org/10.1021/acs.langmuir.1c02724.

14. A. Diallo, L. Rapp, S. Nénon, et al., "Top Gate Copper Phthalocyanine Thin Film Transistors With Laser-Printed Dielectric," *Synthetic Metals* 161, no. 9–10 (2011): 888–893, https://doi.org/10.1016/j.synthmet.2011.02.017.

15. M. Makrygianni, I. Kalpyris, C. Boutopoulos, and I. Zergioti, "Laser Induced Forward Transfer of Ag Nanoparticles Ink Deposition and Characterization," *Applied Surface Science* 297 (2014): 40–44, https://doi.org/10.1016/j.apsusc.2014.01.069.

16. S. Eickelmann, A. Tsouka, J. Heidepriem, et al., "A Low-Cost Laser-Based Nano-3D Polymer Printer for Rapid Surface Patterning and Chemical Synthesis of Peptide and Glycan Microarrays," *Advanced Materials Technologies* 4, no. 11 (2019): 1900503, https://doi.org/10.1002/admt.201900503.

17. P. Sopeña, S. González-Torres, J. M. Fernández-Pradas, and P. Serra, "Spraying Dynamics in Continuous Wave Laser Printing of Conductive Inks," *Scientific Reports* 8, no. 1 (2018), https://doi.org/10.1038/s41598-018-26304-9.

18. L. Rapp, J. Ailuno, A. P. Alloncle, and P. Delaporte, "Pulsed-Laser Printing of Silver Nanoparticles Ink: Control of Morphological Properties," *Optics Express* 19, no. 22 (2011): 21563–21574, https://doi.org/10.1364/OE.19.021563.

19. D. Munoz-Martin, C. Brasz, Y. Chen, M. Morales, C. Arnold, and C. Molpeceres, "Laser-Induced Forward Transfer of High-Viscosity Silver Pastes," *Applied Surface Science* 366 (2016): 389–396, https://doi.org/10.1016/j.apsusc.2016.01.029.

20. E. Dimitriou and N. Michailidis, "Printable Conductive Inks Used for the Fabrication of Electronics: An Overview," *Nanotechnology* 32, no. 50 (2021): 502009, https://doi.org/10.1088/1361-6528/abefff.

21. J. M. Fernández-Pradas and P. Serra, "Laser-Induced Forward Transfer: A Method for Printing Functional Inks," *Crystals* 10, no. 8 (2020): 651, https://doi.org/10.3390/cryst10080651.

22. M. A. Han, H. J. Kim, H. C. Lee, J. S. Park, and H. N. Lee, "Effects of Porosity and Particle Size on the Gas Sensing Properties of SnO2 Films," *Applied Surface Science* 481 (2019): 133–137, https://doi.org/10.1016/j.apsusc.2019.03.043.

23. H. Hu and R. G. Larson, "Evaporation of a Sessile Droplet on a Substrate," *Journal of Physical Chemistry B* 106, no. 6 (2002): 1334–1344, https://doi.org/10.1021/jp0118322.

24. J. Wilkinson, C. Tam, A. Askounis, and S. Qi, "Suppression of the Coffee-Ring Effect by Tailoring the Viscosity of Pharmaceutical Sessile Drops," *Colloids and Surfaces A: Physicochemical and Engineering Aspects* 614, 126144 (2021), https://doi.org/10.1016/j.colsurfa.2021.126144.

25. M. Anyfantakis, Z. Geng, M. Morel, S. Rudiuk, and D. Baigl, "Modulation of the Coffee-Ring Effect in Particle/Surfactant Mixtures: The Importance of Particle–Interface Interactions," *Langmuir* 31, no. 14 (2015): 4113–4120, https://doi.org/10.1021/acs.langmuir.5b00453.

26. Z. Du, H. Zhou, X. Yu, and Y. Han, "Controlling the Polarity and Viscosity of Small Molecule Ink to Suppress the Contact Line Receding and Coffee Ring Effect During Inkjet Printing," *Colloids and Surfaces A: Physicochemical and Engineering Aspects* 602 (2020): 125111, https://doi.org/10.1016/j.colsurfa.2020.125111.

27. Sainsmart. "Sainsmart Website," 2024, https://www.sainsmart.com.

28. Sainsmart. "CNC Model on Sainsmart Website," 2024, https://de.sainsmart.com/collections/cnc/products/sainsmart-genmitsu-3018-pro-cnc-frase.

Supporting Information

Additional supporting information can be found online in the Supporting Information section.